

Nuclear Motions of an Inclusion Complex of Calix[4]arene

B. Paci,[†] M. S. Deleuze,[‡] R. Caciuffo,[†] J. Tomkinson,[§] F. Ugozzoli,^{||} and F. Zerbetto^{*,-}

Istituto Nazionale per la Fisica della Materia e Dipartimento di Scienze dei Materiali e della Terra, Università di Ancona, Via Brece Bianche, 60131 Ancona, Italy, Departement SBG, Limburgs Universitair Centrum, Universitaire Campus, B3590 Diepenbeek, Belgium, ISIS, Rutherford Appleton Laboratory, OX11 0QX Chilton, U.K., Dipartimento di Chimica Generale ed Inorganica, Chimica Analitica e Chimica Fisica, Università di Parma, Viale delle Scienze, 43100 Parma, Italy, and Dipartimento di Chimica "G. Ciamician", Università degli Studi di Bologna, Via F. Selmi 2, 40126 Bologna, Italy

Received: February 4, 1998; In Final Form: June 16, 1998

The 2:1 inclusion complex of *p*-tert-butylcalix[4]arene and *p*-xylene was investigated by a combination of inelastic neutron scattering, INS, experiments and MM3 molecular mechanics calculations. Since the INS spectrum depends only on the vibrational frequencies and the form of the normal modes, the reasonable agreement between experiments and calculations shows that they can be simulated by the MM3 model. Further it validates the use of MM3 to search for possible spectral signatures of a hypothetical 1:1 inclusion complex and for a partial study of the *p*-xylene dynamics within the cage. The latter is accomplished by locating the transition state of a complicated motion of the guest molecule inside the cavity. Transition-state theory is used to calculate the temperature-dependent rate constants, and subnanosecond time scales are obtained.

Introduction

Calixarenes are macrocyclic compounds in which a minimum of three phenols are connected by an equal number of methylenes located in the ortho position to the hydroxyl groups. At least in the smaller, less flexible calixarenes, perfect coplanarity of the rings is never accomplished since it is energetically very unfavorable and the relaxed molecule takes the appearance of a chalice. Conformational interconversion is triggered by tilting a phenyl group, and the relative stabilities of the conformers have been found to depend on the nature of the substituent in the para position to the hydroxyls.¹ Various types of molecular mechanics simulations² have been used successfully to model the energetics observed experimentally by NMR for calix[4]arene.¹ Apart from any interest in the intrinsic dynamics of the molecule, the cavity formed within the molecule springs to mind as a valuable device for the construction of versatile multifunctional materials. The inclusion of a guest molecule within the cage can, in principle, be used either to separate it chemically from other substrates or to tune/shield the properties of the guest. Before such complexation can be used as a synthetic or technological tool, some methods of characterization must be developed and standardized. These methods ought to be able to expose the changes induced in the molecular properties by its inclusion in the cage. The subtlety and the complexity of the phenomenon suggest that such methods must be both experimental and computational. Ideally, the two approaches will complement one another so that their agreement implicitly affords both a deeper insight into the experimental observations and a validation of the theoretical calculations. Furthermore, if the range of the applicability of the experiments differed appreciably from that of the calculations, their partial

overlap would allow the confident extension of either technique. In this work, we assess the joint use of an experimental technique, inelastic neutron scattering, INS, and a computational technique, molecular mechanics, MM3 model.

INS spectroscopy is characterized by limited accessibility (if compared to laboratory techniques that measure similar data, principally infrared, IR, and Raman spectroscopies) and comparatively modest resolution. The value of INS in understanding the vibrational properties of condensed matter can, however, be considerable. The fundamental simplicity of its scattering response implies that an accurate simulation captures well both the structure and the internal force field of the molecule. In fact, the INS cross section is simply related to the atomic displacements and gives a direct measure of the mean-square amplitude for each mode. This is not the case for IR or Raman spectra, where the relationship is less direct. In these optical spectroscopies, the band intensities are also proportional to the dipole moment or to the polarizability tensor surfaces. Information on the atomic displacements is therefore not easily extracted from optical data, because of the changes in the electron distribution induced by the motions themselves. A review of the methods used in the analysis of INS data for molecular vibrations can be found in refs 3 and 4. Some data analysis packages have been written and are commonly used to extract the force constants from the INS intensity distribution.^{5,6} State-of-the-art programs such as CLIMAX⁵ have reached a high level of sophistication and take into account both the presence of higher harmonics and the sharing of the intensity between the parent peak (at the internal mode energy) and the phonon wings (produced by the intermolecular motions^{7,8}). However, the analysis of the vibrational dynamics of complex molecules, with several hundred degrees of freedom, is presently beyond the scope of such programs. (An analysis using CLIMAX was initially attempted for the calix[4]arene(2:1)*p*-xylene but was rapidly identified as unrealistic.) The data analysis presented in this paper is based on a less sophisticated computer program

[†] Università di Ancona.

[‡] Limburgs Universitair Centrum, Universitaire Campus.

[§] ISIS.

^{||} Università di Parma.

⁻ Università degli Studi di Bologna.

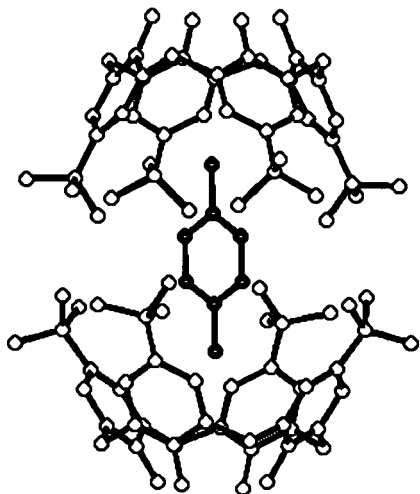


Figure 1. Molecular conformation of the *p*-*tert*-butylcalix[4]arene(2:1)*p*-xylene complex as viewed from the side and perpendicular to the 4-fold axis. The protons are omitted.

that calculates the INS spectrum taking into account only the fundamental internal modes attenuated by thermal motion, but neglects overtones, phonon wings, and combination levels. The starting set of vibrational frequencies and atomic displacements were obtained from molecular mechanics calculations based on the MM3 model,⁹ and no attempt to refine the force field was made. With these limitations, perfect agreement between observed and calculated spectra is certainly not expected. Nevertheless, a reasonable simulation of the INS spectrum can be obtained, giving significant insight into the molecular conformation and the nature of the host–guest potential energy.

Experimental Details

The *p*-*tert*-butylcalix[4]arene(2:1)*p*-xylene complex crystallizes in the tetragonal *P4/n* space group, with room-temperature lattice parameters $a = 12.823(5)$ Å and $c = 25.618(6)$ Å.¹⁰ The guest *p*-xylene molecule is held in a closed cavity formed by two calixarene units facing their *tert*-butyl groups. A side view of the molecular cage, including the guest, is shown in Figure 1. The complex lies on a crystallographic 4-fold axis running along the CH₃–C_{ph} bond of the *p*-xylene.

The neutron experiment was performed using the time-focused crystal analyzer spectrometer TFXA of the ISIS facility at the Rutherford Appleton Laboratory, Oxfordshire, U.K. This is an inverted geometry time-of-flight spectrometer with a white incident beam and final energy (and wavevector k_f) fixed by Bragg reflection from a pyrolytic graphite crystal. Beryllium filters cooled to liquid nitrogen temperature reject higher order Bragg contamination.¹¹ The distribution of detected neutrons is recorded as a function of their total time-of-flight from the source, and since the detected neutrons have the known final velocity, the incident wavevector k_i can be calculated. The intensity measured as a function of time-of-flight is transformed into an intensity as a function of momentum transferred, $\mathbf{Q} = \mathbf{k}_i - \mathbf{k}_f$, and energy transferred, $E = \hbar\omega$, to the sample. More precisely, since the scattering angle ϕ is fixed, the time-of-flight scan corresponds to scanning the component of \mathbf{Q} parallel to the incident beam direction, $Q_{\parallel} = k_i - k_f \cos \phi$, while the perpendicular component, $Q_{\perp} = k_f \cos \phi$, remains constant. The energy transfer is quadratic in the Q_{\parallel} component. This means that TFXA spectra do not provide the energy dependence of the scattering cross section at fixed \mathbf{Q} values but are constrained to a well-defined trajectory in (\mathbf{Q}, E) space, so that for each

energy transfer E there is a corresponding momentum transfer \mathbf{Q} . The simulation procedure must take this fact into account, because the distribution of the intensity from peak to peak and their attenuation are governed by the Debye–Waller factor, which depends on the magnitude of \mathbf{Q} .

The data presented in this paper were collected with a final neutron energy of about 4 meV and at a constant scattering angle ϕ of 133°. The energy transfer range spanned from about 2.5 to 500 meV ($1 \text{ meV} = 8.066 \text{ cm}^{-1}$), covering the complete vibrational range in one spectrum. A polycrystalline sample of about 2 g was prepared at the University of Parma and shown to be single phase by X-ray diffraction. For the neutron experiment, it was mounted into a flat aluminum can in a standard closed cycle refrigerator, and the INS spectra were recorded at $T = 20$ K.

The resolution function of TFXA is characterized by a Gaussian band shape with a full-width-at-half-height (fwhh) that increases monotonically with band position (about 1 meV for $E = 2$ meV and about 5 meV for $E = 200$ meV).

Computational Background

The vibrational scattering function, or double differential cross section, in an inelastic neutron scattering experiment has long been derived by Zemach and Glauber.¹² For an oriented assembly of harmonic oscillators in the form of a single crystal and unpolarized neutrons, it reads

$$\left(\frac{\partial^2 \sigma}{\partial \Omega \partial E} \right)_{\text{inc}} = \frac{1}{4\pi k_i} \sum_L \sigma_{\text{inc}}^L \prod_a \exp \left[-\frac{\hbar}{2m_L \omega_a} (\vec{Q} \cdot \vec{C}_a^L)^2 \coth \left(\frac{\hbar \omega_a}{2k_B T} \right) \right] \times \exp \left(-\frac{n_a \hbar \omega_a}{2k_B T} \right) I_{n_a} \left[\frac{\hbar}{2m_L \omega_a} \frac{(\vec{Q} \cdot \vec{C}_a^L)^2}{\sinh \left(\frac{\hbar \omega_a}{2k_B T} \right)} \right] \delta(E - \hbar \sum_a n_a \omega_a) \quad (1)$$

where Ω is the solid angle, E is the energy transfer, \mathbf{k}_i and \mathbf{k}_f are the incident and scattered neutron wavevectors, σ_{inc}^L is the incoherent neutron scattering cross section of atom L , $\mathbf{Q} = \mathbf{k}_i - \mathbf{k}_f$, is the momentum transfer, \vec{C}_a^L is the displacement vector for atom L in the normal mode a , $\hbar \omega_a$ is the energy of mode a , m_L is the atomic mass, T is the absolute temperature, n_a is the number of quanta transferred in the experiment from mode a , and I_{n_a} is the modified Bessel function. We limit the sum over the atoms to include only the hydrogens which make the largest contribution by far.

The cross section obtained by Zemach and Glauber is valid for single crystals, and a comparison with experimental data obtained for polycrystalline samples requires an average over the random orientations of \mathbf{Q} with respect to the molecular axes. Analytical randomization procedures can only be used in the cases of spherical or the oblate and prolate spheroidal atomic displacement ellipsoids.¹³ Therefore, we adopted a numerical procedure based on the Vegas program¹⁴ for Monte Carlo integration, using Euler angles to generate the random orientations. Convergence required the use of 50 points for the quadrature.¹⁵

The molecular structures were optimized with the MM3 model⁹ using the TINKER suite of programs.¹⁶ The initial geometry was obtained from crystallographic data.¹⁰ After geometry optimization, normal-mode frequencies and atomic

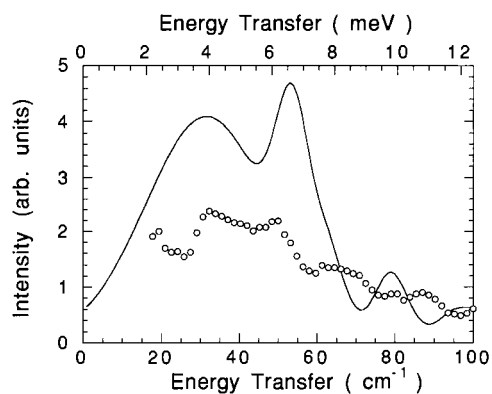


Figure 2. Low-energy region of the inelastic neutron scattering spectrum of the 2:1 inclusion complex of *p*-*tert*-butylcalix[4]arene and *p*-xylene. The solid line represents the convolution of the simulated spectrum with the instrument resolution function.

displacements were calculated. These were used as input for the evaluation of the INS spectra according to eq 1, within the approximations discussed in the Introduction. Results from this computer program were tested against simulations provided by CLIMAX for a simpler system (the dimer of thiophene¹⁷). We were therefore confident that the neutron cross section is correctly calculated. Importantly, MM3 calculations on a series of calix[4]arenes² had successfully reproduced the relative stabilities of the four conformers, including vibrational contributions estimated from normal modes. The search of the transition states was carried out by the algorithm built in the TINKER program, using as starting points a set of geometries generated by performing a coupled series of rotations and tilting of the *p*-xylene molecule. The subsequent calculations of the rate constants were performed by the UNIMOL program¹⁸ and employed the activation energy and the vibrational frequencies calculated by the TINKER program.

Results and Discussion

In this work, we study the vibrational spectrum of the 2:1 inclusion complex of *p*-*tert*-butylcalix[4]arene and *p*-xylene. Individual vibrational modes involve contributions from all the atoms in one or more of the three molecules that form the cluster. In the spectrum, the motion is compounded into a single frequency and intensity. In this sense, vibrational spectroscopy conveys a synoptic image of atomic motions of the molecule. It may be felt that in this process information relevant to individual nuclei is lost. However, INS spectra owe their structure to two properties: first, the form of the scattering vibration; second, a thermal (Debye–Waller) factor. The latter term has contributions from the form of all the vibrations. The reasonable spectral simulation therefore implicitly recovers the information of the nuclear movements contributing to each vibrational mode. Conveniently, inelastic neutron scattering is best suited to study the low- to mid-frequency spectral region where the effects of the guest–host interactions should have their largest impact.

The Spectrum. The experimental inelastic neutron scattering spectrum of the 2:1 inclusion complex of *p*-*tert*-butylcalix[4]arene and *p*-xylene is compared with the results of the simulations in Figures 2, 3, and 4. The scale in the three figures is constant. Notice, however, that in Figures 3 and 4 an offset of 1 for the experimental intensities has been introduced for the sake of clarity. Comparison of the three figures shows that either the low-frequency region (below 80 cm⁻¹) is calculated too intense or the remaining spectrum is calculated with too

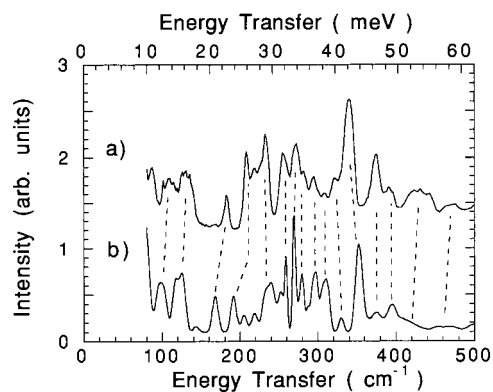


Figure 3. Intermediate-energy region of the inelastic neutron scattering spectrum of the 2:1 inclusion complex of *p*-*tert*-butylcalix[4]arene and *p*-xylene: (a) experimental data; (b) simulated spectrum convoluted with the instrument resolution. A vertical offset has been introduced for the sake of clarity. The assignment of the peaks is indicated by the broken lines.

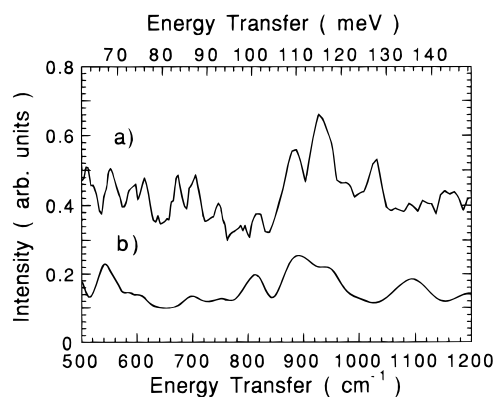


Figure 4. High-energy region of the inelastic neutron scattering spectrum of the 2:1 inclusion complex of *p*-*tert*-butylcalix[4]arene and *p*-xylene: (a) experimental data; (b) simulated spectrum convoluted with the instrument resolution. A vertical offset has been introduced for the sake of clarity.

little intensity. Griffin and Jobic¹⁹ have shown that the low-frequency vibrations may not contribute to the Debye–Waller factor, an event that may effectively increase the intensity of the high-frequency region. Because of the qualitative approach used here, we have not pursued this issue.

Examination of the separate parts of the spectra shows that the overall nature of the response is reasonably well captured by the simulations. The central part, Figure 3, is detailed in Table 1, where the assignments of the strongest lines of the lowest frequency region are given. These assignments are based on visual inspection and were obtained progressively starting from the low-energy region. Three major points emerge:

- (1) Generally there is reasonable agreement between the experimental and calculated bands.
- (2) The relative intensity of some bands is not quantitatively reproduced.
- (3) Some of the calculated bands appear to be split.

The most trivial reason for the intensity redistribution is the imperfect simulation of the contributions made by hydrogen atoms to the molecular motions. Apart from this, two other effects can play a role. The first is disorder in either the environment or the local chemical groups; the second, already mentioned, is the possibility that the Debye–Waller factor is not constructed of contributions from all vibrational motions.¹⁹ Similar considerations can be made for the band splitting with the further possibility, already mentioned above, that the MM3

TABLE 1: Most Prominent Experimental and Calculated Bands (Wavenumbers in cm^{-1}) in the Low-Frequency Region ($80\text{--}520\text{ cm}^{-1}$) of the Inelastic Neutron Scattering Spectrum of the 2:1 Inclusion Complex with *p*-*tert*-Butylcalix[4]arene

experimental	calculated
85	79
100–112	98
126–134	118–124
183	168
208	191
218	205–218
234	235
256	259
271	270
280	280
294	296
311	311
322	330
340	354
375	376
392	395
425, 431, 444	411435
456, 479	460–470

model has a different degree of accuracy for different nuclear motions so that vibrations that are accidentally degenerate in the complex are no longer so in the calculations. In any event, we believe that the less than perfect simulation of the central frequency region of the spectrum is acceptable. The present result concurs with the documented ability of the model to calculate with reasonable accuracy the vibrational frequencies.²⁰

Spectral Markers of the Guest–Host Interactions. The molecular dynamics reflected in the spectral response is determined by the electronic potential energy surface of the supramolecular system. It is usual to expand the potential energy surface (PES) of the molecule as a Taylor series. At the equilibrium geometry the first derivative of the potential energy surface is zero. The second derivatives, or Hessian matrix, can be used to generate the normal modes of vibration and their frequencies. The molecular geometry and the vibrational spectrum are therefore associated with the first two terms of the PES expansion. Although due to the second-order terms, the INS spectrum remains a function of the first order through the influence of geometry. Indeed, different molecular structures may generate different spectra because they are characterized by different normal modes. While there is no doubt that the sample is a 2:1 inclusion compound, spectral evidence of complexation can be found in the form of characteristic spectroscopic markers for this arrangement. In Figure 5, the experimental spectrum is also compared with the simulated INS spectrum of a hypothetical 1:1 inclusion complex of *p*-*tert*-butylcalix[4]arene and *p*-xylene. Better agreement between calculations and experiments is obtained for the 2:1 adduct than the 1:1 adduct. Indeed the low-frequency region located around 200 cm^{-1} is seen to be particularly diagnostic for the 2:1 versus 1:1 complexation. It is instructive to divide that region into three parts. In the central part, the experimentally intense peak at 183 cm^{-1} is assigned to the strong band calculated at 168 cm^{-1} for the 2:1 system. Notice that in the 1:1 complex the same band falls at 161 cm^{-1} , where it is calculated to have much less intensity. In the higher energy region, comparison of the two simulated spectra shows, for the 1:1 adduct, an intensity redistribution which, once more, is in worse agreement with the experiment than for the 2:1 complex. Finally, even the low-energy region, below the central band of 183 cm^{-1} , is better reproduced by the calculations performed on the 2:1 complex. Here the simulations find that the 1:1

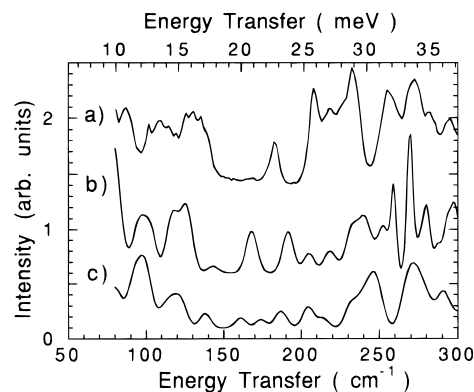


Figure 5. Comparison between the experimental spectra (a) and the simulations for a 2:1 inclusion complex (b) and a 1:1 inclusion complex (c) of *p*-*tert*-butylcalix[4]arene and *p*-xylene.

complex has excessive intensity at about 138 cm^{-1} , in contrast to the experiments.

To better understand the differences between the spectra of the two adducts, we plotted the normal modes of the two systems. In general, the differences were not sufficient to allow for a visual approach to the intensity redistribution. However, in the low-energy region it was noticed that the most active vibrational mode of both the 1:1 and 1:2 complexes was mainly concentrated on the guest molecule (see Figure 6). It is now easy to rationalize the difference between the two simulated spectra. The calix[4]arene cage makes the largest contribution to the INS intensity; the ratio between the spectral contribution of the host(s) versus the guest is the same as the molecular ratio in the complexes. When only one cage is present, the vibrations localized on the *p*-xylene moiety appear to increase their intensity. In a sense, it is rather surprising that there are not more “diagnostic” bands. The requisites for the existence of these bands are two: first, the vibrations must be localized on the guest molecule; and second, their frequencies must fall in a region where transitions of the calixarene are not intense. Further analysis of the normal modes showed why it was possible to locate only one such band. The interaction between the guest and the host is sufficiently strong that the vibrations are delocalized over both the guests and host(s) such that very few diagnostic bands fall in unencumbered regions of the spectrum.

We conclude this subsection by noting that the present procedure can discern between the two different complexation schemes, 1:1 and 1:2. We believe that this conclusion is reasonable, notwithstanding the need to support it by further experimental work.

Guest–Host Dynamics. The molecular mechanics based simulations of INS spectra are a convenient starting point to introduce what is probably one of the most interesting parts of the dynamics of the system. This is the set of intracavity motions of *p*-xylene. In the previous subsection, it was shown that both the experimental spectrum and the calculations point toward a picture in which the vibrational motions are, in the most part, delocalized over the cages and the guest molecule. These motions are quite complicated and have recently been modeled as a combination of methyl motions plus a sinusoidal displacement of *p*-xylene inside the cavity.²¹ Here, we have tried to explore the potential energy surface and locate stationary points for the *p*-xylene motion. Before proceeding, a cautionary note is in order: this task was not easy and such transition states are characterized by extremely low frequencies and activation barriers. The results should, therefore, be taken as a further,

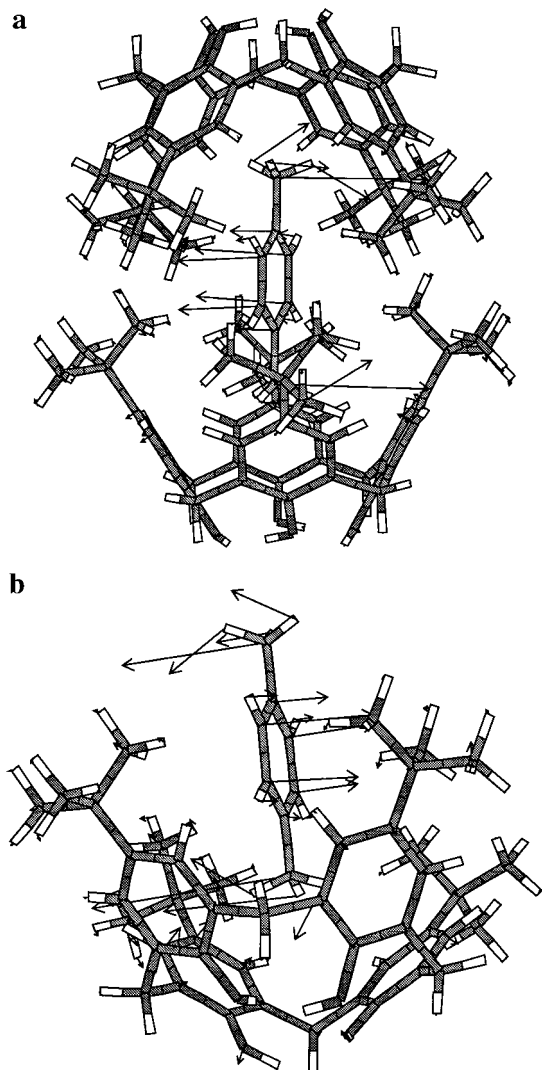


Figure 6. Schematic diagrams of two vibrational motions of the complexes (a) for the 143 cm^{-1} band of the 2:1 adduct (which, in agreement with observation, has little intensity) and (b) for the 138 cm^{-1} band of the 1:1 adduct (which, contrary to observation, has a sizable intensity).

but limited, contribution toward our understanding of the complicated dynamics of *p*-xylene inside the cage formed by two calix[4]arenes. The default search algorithm of Tinker was able to locate a number of transition states for the hydroxyl group torsions. Only one of these states described a complicated rearrangement of *p*-xylene and the calix[4]arene cages, and this is the transition state shown in Figure 7. Also shown in the figure is the vector describing the molecular displacement which returns the complex to the minimum.

It is difficult to assess the structural arrangement of Figure 7 in absolute terms. However, inspection shows that the transition-state geometry is of low symmetry. The local symmetry axes of the two cages no longer coincide with that of the *p*-xylene, and the normal mode with the imaginary frequency is highly nonsymmetric. Indeed such mode involves a complex relative displacement of the cages and the *p*-xylene. In this displacement, the guest executes an anti phase libration of the phenyl ring of *p*-xylene against its two methyl groups. This is essentially the same kind of motion that has been successfully used elsewhere²¹ to describe the quantum rotational dynamics of the *p*-xylene methyl groups in the low-energy region (between 1 and 20 cm^{-1}). The host displacement consists of a number of *tert*-butyl torsions in one of the cages plus the tipping of the

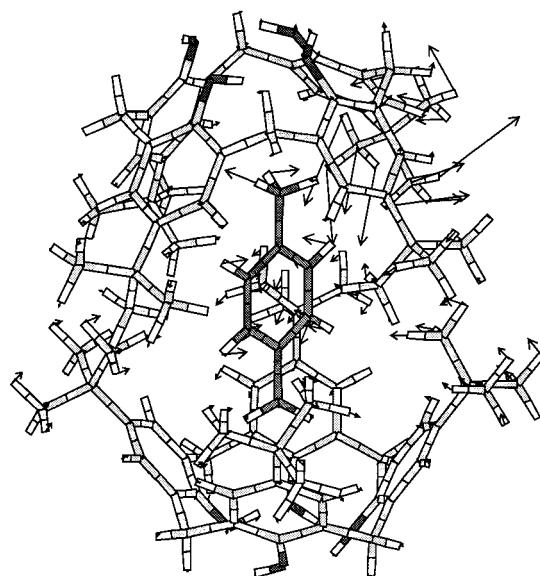


Figure 7. Transition-state rotation of *p*-xylene inside the cavity in its 2:1 inclusion complex with *p*-*tert*-butylcalix[4]arene. This motion is characterized by an imaginary frequency.

TABLE 2: $\log_{10}(K)$ Calculated Rate Constants, s^{-1} , for the Motion of *p*-Xylene Associated with the Transition State Shown in Figure 6

T (K)	$\text{CH}_3\text{C}_6\text{H}_4\text{CH}_3$ $\log_{10}(K)$	$\text{CH}_3\text{C}_6\text{D}_4\text{CH}_3$ $\log_{10}(K)$	variation (%)
50	10.316	10.274	-9.2
100	11.082	11.079	-0.8
150	11.342	11.350	2.7
200	11.477	11.494	4.0
250	11.559	11.580	5.0
300	11.615	11.638	5.6

whole of the second calix[4]arene cage. The imaginary frequency associated with this motion is 19.7 cm^{-1} and is hardly changed in the case of its d_4 isotopomer, 19.3 cm^{-1} . This isotopomer was produced by exchanging only the hydrogen atoms of the phenyl group.

The calculated energy barrier for the transition state is 0.41 kcal/mol . If one includes the zero-point energies, this falls to 0.30 kcal/mol for the protonated system and 0.32 kcal/mol for the isotopomer. The further calculation of the entropic contributions based on the harmonic approximation gives $\Delta S^\ddagger = -5.27\text{ cal/mol}$. With these values we determine $\Delta G_{273}^\ddagger = 1.74\text{ kcal/mol}$, for the protonated system and $\Delta G_{273}^\ddagger = 1.75\text{ kcal/mol}$ for the isotopomer.

The picture that emerges for this interesting low-frequency motion is that it destroys the molecular symmetry and it pertains to *p*-xylene but is highly contaminated by cage motions. The motion is now sufficiently well characterized to enable future experimental identification. However, we re-emphasize that this is only one of the possible transition-state motions and that because of the complexity of the system there may be more of such points.

To add further insight and with a view to possible experimental identification, we also calculated the associated rate constants at several temperatures. The scheme used was based on transition-state theory,¹⁸ and the results are given in Table 2. The rationale for the extension of the present study is that transition-state theory,¹⁸ which yields kinetics rate constants, employs some of the quantities that were used in the INS simulation. These are the vibrational frequencies of the complex. They must be compounded with the vibrational

frequencies of the transition state and the energy difference between these two stationary points. The rate constants are reported for the protonated guest and for the isotopomer. It was found that the time scale of motion described above is in the subnanosecond regime. The complexity of the motion of *p*-xylene inside the cage is emphasized by the last column of Table 2, where the variation of the rate constant with the temperature for the two isotopomers is reported. At low temperatures the process is slightly slower for the deuterated system. This occurs because the barrier is increased by 0.015 kcal/mol when zero-point energies are included. At higher temperatures, on the contrary, the process is faster in the deuterated compound, an effect that is likely to be due to a redistribution of the zero-point energies.

Conclusion

The combination of inelastic neutron scattering spectroscopy and spectral simulations based on molecular mechanics calculations can be an effective tool to retrieve information on the nuclear dynamics and the weakly bonding interactions that characterize large supramolecular systems. The simulation of the experimental spectrum validates the computational model and justifies its extension to explore other properties of the system. It was shown that the inelastic neutron scattering spectrum of the 2:1 inclusion complex of *p*-*tert*-butylcalix[4]-arene and *p*-xylene presents a different signature from that of a hypothetical 1:1 complex. This signature is due to an intensity redistribution of some vibrational bands, but more importantly, to the presence of an intense band associated with *p*-xylene only. Furthermore, it was shown that the intracavity motion of *p*-xylene is a highly complicated process whose components can be mixed with low-frequency motions of the two cages. One such motion was identified and the associated rate constants were calculated at several temperatures for future experimental work.

Acknowledgment. F.Z. gratefully acknowledges partial financial support from the University of Bologna project "Innovative Materials" and MURST project "Supramolecular Devices".

References and Notes

- (1) Harada, T.; Rudzinski, J. M.; Shinkai, S. *J. Chem. Soc., Perkins Trans 2* **1992**, 2109.
- (2) Harada, T.; Rudzinski, J. M.; Osawa, E.; Shinkai, S. *Tetrahedron* **1993**, *49*, 2109. Fischer, S.; Grootenhuis, P. D. J.; Groenen, L. C.; van Hoorn, W. P.; van Veggel, F. C. J. M.; Reinhoudt, D. N.; Karplus, M. *J. Am. Chem. Soc.* **1995**, *117*, 1611.
- (3) Kearley, G. J. *Nucl. Instrum. Methods Phys. Res. A* **1995**, *354*, 53.
- (4) Kearley, G. J. *Spectrochim. Acta* **1992**, *48A*, 349.
- (5) Kearley, G. J. *J. Chem. Soc., Faraday Trans. 2* **1986**, *8*, 41.
- (6) Li, J.-C.; Leslie, M. *Nucl. Instrum. Methods Phys. Res. A* **1995**, *354*, 66.
- (7) Kearley, G. J.; Tomkinson, J.; Penfold, J. *Z. Phys.* **1987**, *B6*, 67.
- (8) Tomkinson, J.; Kearley, G. J. *J. Chem. Phys.* **1989**, *9*, 5164.
- (9) Allinger, N. L.; Yuh, Y. H.; Lii, J.-H. *J. Am. Chem. Soc.* **1989**, *111*, 8551. Lii, J.-H.; Allinger, N. L. *J. Am. Chem. Soc.* **1989**, *111*, 8566. Lii, J.-H.; Allinger, N. L. *J. Am. Chem. Soc.* **1989**, *111*, 8576.
- (10) Andreetti, G. D.; Ugozzoli, F.; Vicens, J.; Böhmer, V. *Calixares*; Kluwer Academic Publishers: Dordrecht, 1991.
- (11) Penfold, J.; Tomkinson, J. Internal Report No. RAL-86-019; Rutherford Appleton Laboratory: Chilton, U.K., 1986.
- (12) Zemach, A. C.; Glauber, R. *J. Phys. Rev.* **1956**, *101*, 118.
- (13) Tomkinson, J.; Warner, M.; Taylor, A. D. *Mol. Phys.* **1984**, *51*, 381.
- (14) Press, W. H.; Teukolsky, S. A.; Vetterling, W. T.; Flannery, B. P. *Numerical Recipes*, 2nd ed.; CUP: New York, 1992. Lepage, G. P. *J. Comput. Phys.* **1978**, *27*, 192.
- (15) Hudson, B.; Warshel, A.; Gordon R. G. *J. Chem. Phys.* **1974**, *61*, 2929.
- (16) Dudek, M.; Ponder, J. *J. Comput. Chem.* **1995**, *16*, 791. Kundrot, C.; Ponder, J.; Richards, F. *J. Comput. Chem.* **1991**, *12*, 402.
- (17) Degli Esposti, A.; Zerbetto, F. *J. Phys. Chem. A* **1997**, *101*, 7283.
- (18) Gilbert, R. G.; Smith, S. C. *Theory of unimolecular and recombination reactions*; Blackwell Scientific Publications: Oxford, 1990.
- (19) Griffin, A.; Jobic, H. *J. Chem. Phys.* **1981**, *75*, 5940. Jobic, H.; Ghosh, R. E. *J. Chem. Phys.* **1981**, *75*, 4025.
- (20) Allinger, N. L.; Chen, K.; Lii, J.-H. *J. Comput. Chem.* **1996**, *17*, 642.
- (21) Schiebel, P.; Amoretti, G.; Ferrero, C.; Paci, B.; Prager, M.; Caciuffo, R. *J. Phys. Condens. Matter* **1998**, *10*, 2221.